CFD modelling of the boundary layer in complex terrain validated by field measurements

Jochem Vermeir, Mark Runacres, Tim De Troyer
Fluid mechanics and Thermodynamics Research group (FTRG)
Department of Industrial sciences and technology
Erasmushogeschool Brussel
Nijverheidskaai 170, Brussels 1070, Belgium

March 11, 2012

1 Abstract

A numerical study of the combined implementation of terrain roughness and velocity shear of the atmospheric boundary layer is presented in this paper. The consistency of these boundary conditions is tested by simulating the flow over a flat terrain. The results are described in the first part of this paper. Once these conditions are tuned, they are applied to perform a siting study on a complex terrain. The complexity of the terrain for this paper is due to buildings and obstacles, but the proposed method can also be applied for complex terrain topography. From the siting study, a suitable location to perform a resource assessment is derived. Validation is performed by comparing the results of the numerical siting study with field measurements. The CFD (Computational Fluid Dynamics) code used for the research in this paper is OpenFoam 2.0.x.

Keywords: Siting; Complex terrain; Computational Fluid Dynamics; Atmospheric boundary layer; Terrain roughness; Roughness length; Validation; Field measurements;

2 Introduction

A major challenge in numerical siting studies over complex terrain is getting the atmospheric boundary layer right [1]. This boundary layer can be constructed in two ways. By setting a wind profile at the inlet boundary, or by applying a wall function to the ground to fix the wind profile above. These two boundary conditions are complementary and can be used together. The difficulty is that these two boundary conditions satisfy different equations that are not necessarily consistent. The inlet profile is set by 2 parameters, the friction velocity U^* and the roughness length z_0. The wall function is also determined by 2 parameters, the roughness height K_s and the roughness constant C_s. They are related by the roughness length z_0: as a rule of thumb, $K_s = 20z_0$.

The functions described above will be used to demonstrate how the two boundary conditions can be tuned for simultaneous use. This type of roughness implementation is currently available in the CFD code OpenFoam 2.0.x and a number of other CFD codes. The solver that we use for this paper is SimpleFoam. It is a steady-state solver for incompressible turbulent flow, using a semi implicit method for pressure-linked equations. The solver allows to couple the Navier-Stokes equations with an iterative procedure. The selected Reynolds Averaged Stress (RAS) turbulence model is the k-ϵ model.

We first discuss the implementation of the atmospheric boundary layer on a flat terrain. The results are then applied to a siting study on an existing complex terrain. The study is finally validated with on-site measurements.

3 Numerical simulation of the atmospherical boundary layer on a flat terrain

The two ways of setting the boundary layer are first studied separately and then applied together, on a flat terrain. Using the wall function only, a uniform inlet velocity will be turned into a logarithmic wind profile as it evolves over the surface. The value for the (constant) flow velocity at the inlet is chosen to be the mean wind velocity of the wind profile we expect to see based on the applied parameters of the wall function. In this way the total flow remains constant over the surface. Our results show that the error between the simulated profile and the expected profile is less than 5 %. Variation of the roughness constant has a major influence on the error, especially for lower heights. A constant value of 0.327 is chosen for C_s, which gives the best result. The relationship between K_s and z_0 and the value for C_s is based on data in the literature [2].

A second test consists of applying an atmospheric boundary layer profile at the inlet and a slip boundary condition on the surface. The wind profile at the inlet is given by [3]:

$$U(z) = \frac{U^*}{\kappa} \ln(\frac{z + z_0}{z_0}) \quad (1)$$

where

$U*$ is the friction velocity [m/s]

κ is the Von Karman coefficient wich is 0.41

z is the vertical height coordinate [m]

z_0 is the roughness length [m]

The profile at the outlet of the case has exactly the expected profile. Combining both boundary conditions, it should be possible to set up a logarithmic wind profile that remains constant when moving over the surface (with wall function applied). If so, both boundary conditions are consistent and representative of the atmospheric boundary layer. A result for this simulation is shown in figure 1, where the wind profile at the outlet is compared with the expected profile (i.e. the profile at the inlet). The deviation between the curves is small. The maximum error is reached at the end of the curve (or for bigger heights) and is approximately 5%. The deviation at the end of the curve is caused by the continuity of the flow.

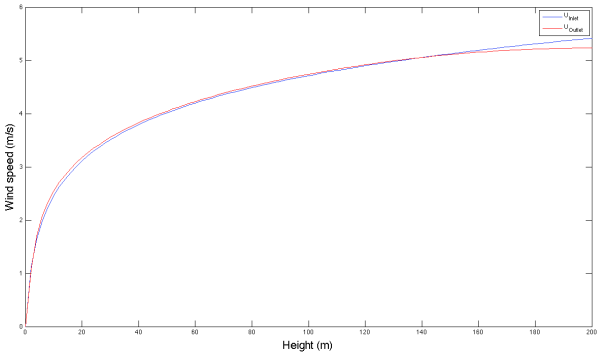

Figure 1: Simulated wind profiles at inlet and outlet of the case.

4 Siting study in complex terrain

After tuning both boundary conditions, we apply them to a siting study on an existing terrain. First the modelling of the terrain is described. In a next step the method for the implementation of the boundary conditions is described. Finally the results of the numerical simulations are shown.

4.1 Modeling the terrain

In this case the complexity of the terrain is due to buildings and obstacles. Terrain topography such as hills can be treated in the same way. We have measured the building and obstacles with a total station. The size of the domain and the amount of obstacles and buildings taken into account for the 3D model are based on rules of thumb. These rules describe the size of the recirculation zone and wake effects on a 2D obstacle. They describe the distance before the wind speed reaches the free stream velocity again and

are available in the literature [4]. Data from the total station and terrain topography from Google Earth are combined into a 3D model of the site. This model is then introduced in the CFD code as a 3D surface. The site is located near Antwerp in Belgium. The 3D model of the terrain is shown in figure 2.

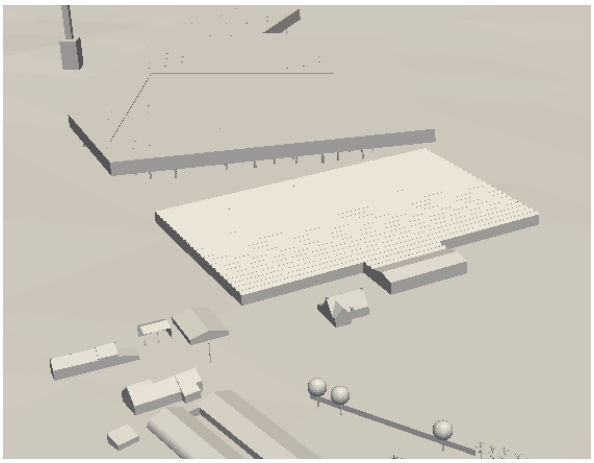

Figure 2: 3D model terrain

4.2 Estimation of the boundary conditions

To estimate the inlet conditions for the numerical simulation, data from a nearby measurement station (Woensdrecht, Netherlands) are used. Long-term data over approximately 12 years are used to determine the dominant wind direction. In figure 3 the frequency of winds over a long time period is plotted per wind direction.

Southwest is clearly the dominant wind direction and should certainly be simulated in the siting study. Another figure that can be derived from the measurements of the weather station is figure 4. This figure shows the mean wind speed per wind direction in a polar graph. Other wind directions for the numerical study can be derived from the plot. The first step to estimate the inlet conditions is to use these mean wind speeds for the simulations.

As data from the measurement station are only available at one height, the roughness length of the

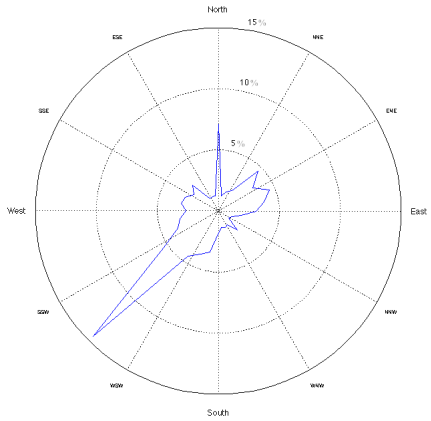

Figure 3: Wind rose with frequency of occurence

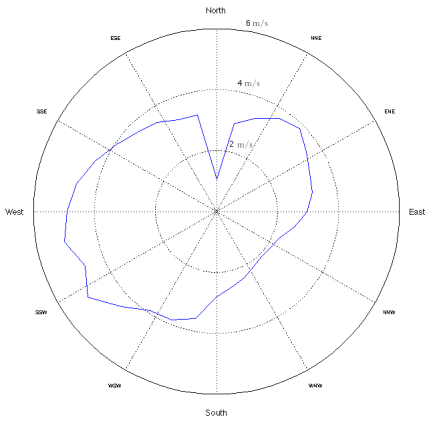

Figure 4: Wind rose with mean wind speed

terrain can't be estimated using equation (1). Therefore the roughness length has to be estimated. Tables with roughness lengths for each type of vegetation, height of and spatial area between buildings are present in the literature [5]. These two steps are then repeated for every simulated wind direction. With the estimate of the roughness length and the mean wind speed from the nearby measurement station, the friction velocity $U^*$and thus the wind profile at the inlet can be calculated using equation (1). In a next step the turbulence parameters are calculated.

The turbulent kinetic energy k can be derived from equations available in the literature [6]:

$$k = \frac{(U^*)^2}{\sqrt{C_\mu}} \tag{2}$$

where C_μ is a $k - \epsilon$ parameter whose value is typically given as 0.09. An equation for the turbulent dissipation rate ϵ is also available in the literature [6]:

$$\epsilon(z) = \frac{(U^*)^3}{\kappa(z + z_0)} \tag{3}$$

4.3 Application on siting study

A siting study is performed to install a small-scale wind turbine next to a farm on the terrain. The owner of the farm does not own all the terrain taken into account for the siting study, so only a small zone of the terrain is used to determine the location of installation. The regulations in Belgium allow a maximum hub height for small wind turbines of 15 m so only this height is investigated. As described in the section above, the boundary conditions are derived from measurement data from a nearby weather station. The analysis of the data showed that west and southwest are two obvious directions since these two directions contain the most energy. The south wind direction is not simulated because no obstacles are located upstream of the zone of interest and therefore the unperturbed wind can be used. Due to the shape and complexity of the terrain, a simulation of the northeast wind direction is also required. The results of these 3 simulations are then combined to derive a good location to install a wind turbine (or in this case to put a measurement station to check the resources on site).

In figure 5 a result of the simulation of the southwest wind is shown. The figure shows a slice plot at a height of 15 m. The area between the black lines shows a region where the wind speed is high in the zone of interest. This region is then used to determine a suitable area for a simulation of the northeast wind. This process is repeated for a simulation of the west wind. A result of the simulation of the northeast wind is shown in figure 6. A large region in the zone of interest has relatively low wind speeds, but a small region has much better wind speeds.

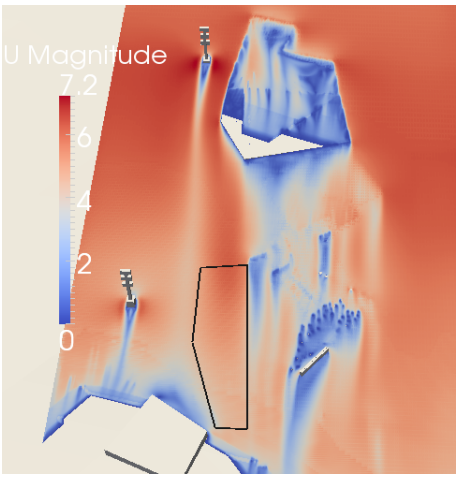

Figure 5: Simulation of the southwest wind

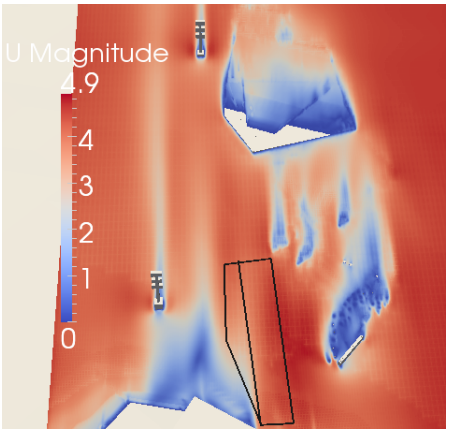

Figure 6: Simulation of the northeast wind

If we take a look at the last simulation in figure 7, it seems on first sight, that no interesting regions for this wind direction can be derived. However a closer look reveals (in figure 8) two regions with a smaller distortion. The two most suitable locations are indicated with a circle.

The simulations show a nearly undisturbed flow the

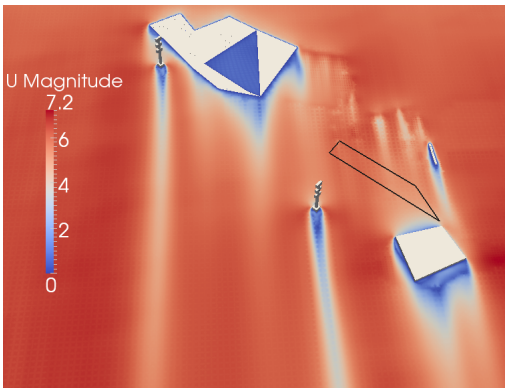

Figure 7: Simulation of the west wind

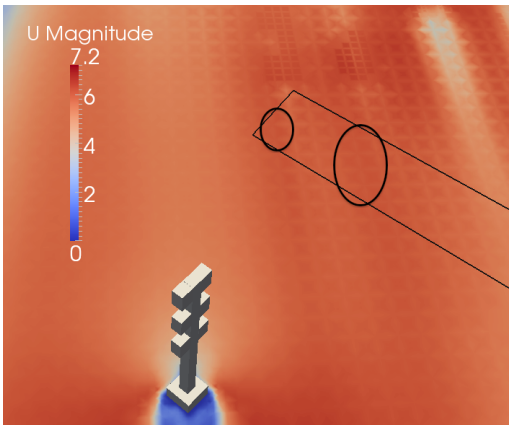

Figure 8: Suitable locations indicated on the simulation of the west wind

southwest and northeast wind direction. The west wind direction even shows a small acceleration of the wind. A feasibility study must be performed. This is done by assessing the resources in the region of interest.

Another aspect in this kind of simulations is the turbulence. The streamlines in the interesting regions can be plotted to give an idea of the turbulence. Zones where the turbulence is high, are not appropriate to install a wind turbine. These conditions will have a negative effect on the lifetime of the turbine (due to fluctuating loads on the blades). The streamlines are investigated in the most interesting region for every wind direction, and this showed that the turbulence was low. An example of a plot of the streamlines for the west wind is shown in figure 9.

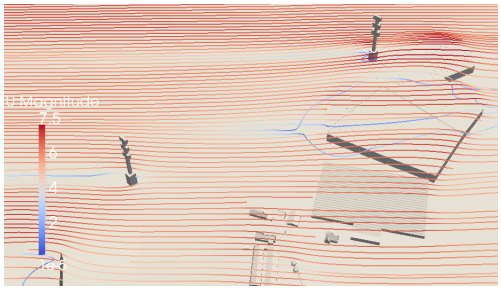

Figure 9: Stream lines at a height of 15 m

4.4 Discussion

With the results of the siting study and practical positioning on the terrain, a location is chosen to install a mast with 2 cup anemometers at different heights (one at 15 m, one at 10.5 m) on the terrain. In figure 10 the variation of the wind speed as a function of the distance perpendicular to the mea n flow at a height of 15 m for the southwest and northeast wind is plotted in a graph. The position of the mast is indicated with a circle on the graph. This is repeated for a simulation of the west wind in figure 11. The Interruption in this figure is due to terrain obstacles.

The wind speed at the position of the top anemometer in the simulation is then compared to the wind speed at the inlet. In table 1 this comparison is shown. The table shows that the distortion of the flow due to buildings is rather low. Only for the west wind a small increase compare to the wind speed at the inlet can be seen.

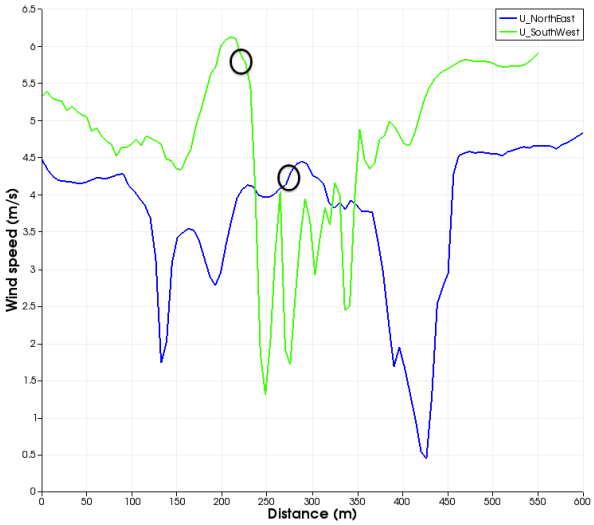

Figure 10: Variation of the wind speed at a height of 15 m in the simulation of the southwest (top line) and northeast (bottom line)

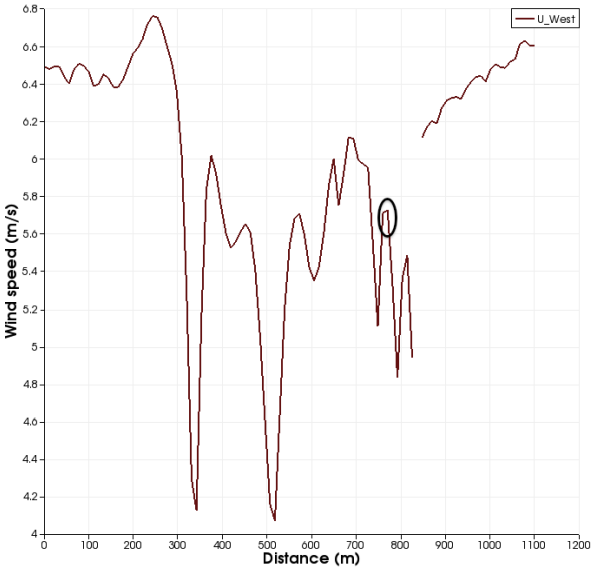

Figure 11: Variation of the wind speed at a height of 15 m in the simulation of the west wind

Table 1: Comparison

Wind direction	Top mast	Inlet	Increase
West	5.59 $\frac{m}{s}$	5.57 $\frac{m}{s}$	0.3 %
Southwest	5.70 $\frac{m}{s}$	5.87 $\frac{m}{s}$	-2.9 %
Northeast	4.32 $\frac{m}{s}$	4.43 $\frac{m}{s}$	-2.5 %

5 Validation

5.1 Method

The goal of these siting studies is to determine the best location to install a small wind turbine. To test the accuracy of the predictions, CFD Simulations need to be validated against field measurements. In a first step, we have determined the parameters for the implementation of the boundary layer at the inlet of the simulation. These are determined by measuring the wind speed at 2 different heights (15 m and 10.5 m) on the same location on the terrain by the use of 2 cup anemometers. The location of the mast is chosen with care. If a certain wind direction (for this validation the west wind simulation is used) is simulated, the mast should obviously be placed in front of the terrain and the flow should be nearly undisturbed.

Next, a second measurement mast is installed on the terrain using the results of the siting study above. The mast is placed in a zone where the turbulence was low and a small acceleration of the wind was predicted.

To validate the simulations, the measured boundary layer is implemented in the simulation and the simulated wind speed on the position of the second mast is determined from the simulation. These results are compared with the field measurements at the second mast.

5.2 Field measurements

The measurement period is set to 2 weeks. We have chosen this period because an adequate estimate of the inlet parameters has to be made. Due to the variability of the wind speed and direction at these low heights, a few hours would not suffice to make a good estimate. The inlet parameters can be calculated from the measurements using equation (1). If

the wind speed is measured at two different heights, both parameters can be calculated by the use of equation (1). This equation can be used for both heights, which are both known (15 m and 10.5 m) :

$$U_1(z_1) = \frac{U*}{\kappa} \ln(\frac{z_1 + z_0}{z_0}) \tag{4}$$

$$U_2(z_2) = \frac{U*}{\kappa} \ln(\frac{z_2 + z_0}{z_0}) \tag{5}$$

From the equations above we find:

$$\frac{U_1(z_1)}{U_2(z_2)} = \frac{\ln(\frac{z_1+z_0}{z_0})}{\ln(\frac{z_2+z_0}{z_0})} \tag{6}$$

The roughness length z_0 is determined using a root finding algorithm. The friction velocity can then be determined with:

$$U^* = \frac{U_1(z_1) * \kappa}{\ln(\frac{z_1+z_0}{z_0})} = \frac{U_2(z_2) * \kappa}{\ln(\frac{z_2+z_0}{z_0})} \tag{7}$$

5.3 Results

The method described in the section above is a well known method for validating siting studies with field measurements at larger heights [8]. These siting studies are usually performed to install large MW wind turbines on the simulated terrain. When comparing the field measurements with siting studies for MW wind turbines an averaging period of 10 minutes is used. For lower heights methods are available in the literature explaining the validation of CFD simulations with wind tunnel experiments for the built environment [7]. Methods for the validation of CFD simulations with field measurements at lower heights are not yet present in the literature. Due to the variability of the wind speed and direction at lower heights a smaller averaging period and a 10 minute averaging period is used to validate the simulations. The results of both periods are than compared.

As described in the section above the undisturbed wind is measured on the terrain at 2 heights to estimate the inlet parameters (this will be called mast 1). Two different averaging period (1 minute and 10 minute intervals) of the field measurements are used to determine these parameters. In table 2 these parameters are shown. Both sets of parameters are applied to perform the simulations.

Table 2: Inlet parameters

Interval	1 minute	10 minutes
Top anemometer	5.4 $\frac{m}{s}$	4.8 $\frac{m}{s}$
Lower anemometer	4.8 $\frac{m}{s}$	4.2 $\frac{m}{s}$
Roughness length	1.03 m	1.38 m
Friction velocity	0.81 $\frac{m}{s}$	0.78 $\frac{m}{s}$

A second measurement mast with 2 anemometers is placed on the most suitable location (based on the siting study) on the terrain (mast 2). The distance between both masts is measured using a total station. This distance is taken into account to make a time shift between the wind speed measured at mast 1 (i.e. inlet) and mast 2. As the wind speed is lower on the lower anemometer, different time shifts are used. The measurements from mast 2 are then compared to the numerical simulations. The two different averaging periods are presented in the next two tables. The first table 3 shows the results for an averaging period of 1 minute. Table 4 shows the results for an averaging period of 10 minutes.

Table 3: Validation with averaging period 1 minute

Height	15 m	10.50 m
Field Measurement	5.68 $\frac{m}{s}$	5.22 $\frac{m}{s}$
Simulation	5.93 $\frac{m}{s}$	5.15 $\frac{m}{s}$
Error	4.2 %	1.3 %

Table 4: Validation with averaging period 10 minutes

Height	15 m	10.50 m
Field Measurement	4.78 $\frac{m}{s}$	4.15 $\frac{m}{s}$
Simulation	5.35 $\frac{m}{s}$	4.68 $\frac{m}{s}$
Error	10.6 %	11.3 %

5.4 Conclusions

The validation results for the averaging period of 1 minute appears to be better than for the averaging period of 10 minutes. This can be explained by the

variability of the wind at these low heights. In the averaging period of 10 minutes the variability in wind direction and wind speed will be higher, and therefore the error between the measured and the simulated wind speeds will be larger.

Results also show for an averaging period of 1 min, that the wind is indeed accelerated on terrain at mast 2. This is confirmed by both the measurements and the simulation. This is shown in table 5. When the adopted averaging period is larger, a clear deviation between the field measurements and the simulation is present. This phenomenon will be studied in the future.

Table 5: Validation results averaging period 1

Height	Mast 1	Mast 2	Acceleration
15 m	5.4 $\frac{\mathrm{m}}{\mathrm{s}}$	5.68 $\frac{\mathrm{m}}{\mathrm{s}}$	5.2 %
10.5 m	4.8 $\frac{\mathrm{m}}{\mathrm{s}}$	5.22 $\frac{\mathrm{m}}{\mathrm{s}}$	8.8 %
Height	Inlet	Simulation	Acceleration
15 m	5.4 $\frac{\mathrm{m}}{\mathrm{s}}$	5.93 $\frac{\mathrm{m}}{\mathrm{s}}$	9.8%
10.5 m	4.8 $\frac{\mathrm{m}}{\mathrm{s}}$	5.15 $\frac{\mathrm{m}}{\mathrm{s}}$	7.3 %

6 Summary and conclusions

In this study, numerical experiments were carried out using the CFD code OpenFOAM. The numerical experiments consist of applying a wall function on a flat terrain and an atmospheric boundary layer at the inlet. The goal of this first experiment was to make the wall function and the inlet consistent. This resulted in a logarithmic wind profile that remains constant when moving over the surface. When comparing the inlet and the outlet of the case, a maximum error of 5% was found. This showed that both conditions are consistent and representative of the atmospheric boundary layer.

After tuning both boundary conditions, they are applied on an existing terrain to perform a siting study. The inlet conditions for this study are estimated using long-term wind data from a nearby measurement station. The long-term data showed 2 most relevant wind directions to simulate in the siting study. An extra wind direction is required due to the complexity of the terrain. This siting study showed an interesting location on the terrain to install a small-scale wind turbine. To investigate the resources a measurement station was installed on the location.

Finally the results of the siting study are validated using an extra measurement station installed on the terrain. In this paper different averaging periods for the field measurements are tested to validate the simulations. The averaging period of 1 minute appears to give better results. Validation showed an error of less than 5 % between the results of the CFD simulations and the field measurements. In other words the accuracy of the predictions done in the CFD simulations is good. The validation also show that a suitable location can be chosen based on the siting study. An acceleration on the location is confirmed by both the field measurements and the numerical simulations.

7 Acknowledgements

The work described in this paper was partially funded by IWT (Institute for Flanders Innovation for Science and Technology) and ERDF (European Regional Development Fund).

References

[1] Blocken B, Stathopoulos T, Carmeliet J. 2007. *CFD simulation of the atmospheric boundary layer: wall function problems.*, Atmospheric Environment 41(2): 238-252. Elsevier.

[2] Ligrani P, Moffat R, 1986. *Structure of transitionally rough and fully rough turbulent boundary layers* Journal of fluid mechanics 162, 69,98. Cambridge University Press.

[3] Richards P, Hoxey, R, 1993. *Appropriate boundary conditions for computational wind engineering models using the k-ϵ turbulence model.* Journal of Wind Engineering and Industrial Aerodynamics, 46,47, 145-153. Elsevier.

[4] Wegley H, Ramsdell J, Orgill M, Drake R, 1980. *Siting Handbook for Small Wind Energy Conversion Systems.*

[5] Wieringa J, 1992. *Updating the Davenport roughness classification.*, Journal of Wind Engineering and Industrial Aerodynamics 41-44, 357-368. Elsevier.

[6] Wilcox D 1993, *Turbulence modelling for CFD*, DCW Industries, California.

[7] Wallbank T, 2008. *WindSim validation study*, Windsim, Tønsberg, `http://tinyurl.com/7xbcdar` (November 25, 2011)

[8] Willemsen E, Wisse J. 2002. *Accuracy of assessment of wind speed in the built environment*, Journal of Wind Engineering and industrial Aerodynamics 90, 1183-1190. Elsevier.